Suppression of Coherence Collapse in Semiconductor Fano Lasers

Thorsten S. Rasmussen,* Yi Yu,† and Jesper Mork‡
DTU Fotonik, Technical University of Denmark, DK-2800 Kongens Lyngby, Denmark

(Received 15 July 2019; published 3 December 2019)

We show that semiconductor Fano lasers strongly suppress dynamic instabilities induced by external optical feedback. A comparison with conventional Fabry-Perot lasers shows orders of magnitude improvement in feedback stability and in many cases even total suppression of coherence collapse, which is of major importance for applications in integrated photonics. The laser dynamics are analyzed using a generalization of the Lang-Kobayashi model for semiconductor lasers with external feedback, and an analytical expression for the critical feedback level is derived.

DOI: 10.1103/PhysRevLett.123.233904

Nonlinear dynamical systems with time-delayed feedback show rich and varied physics due to their infinite-dimensional nature [1] with important examples in a large variety of disciplines, such as mechanics [2], physiology [3], and neural networks [4]. Semiconductor lasers with external optical feedback are one of the most studied examples of such delay systems, due to their wide range of applications and the serious issue of instabilities, chaos, and coherence collapse arising from even extremely weak feedback [5–9]. The inherent sensitivity of these lasers toward external feedback as well as the nature of the nonlinear dynamics remain open problems under study [10–14], and the instabilities are a particularly relevant issue in on-chip applications, due to the absence of integrated optical isolators. This has led to a number of novel solution proposals, e.g., isolators based on topological photonics [15,16], reduction of the alpha factor [12,17], increased damping [12], and complicated laser geometries [14]. Most studies have dealt with macroscopic lasers, while the feedback dynamics of emerging microlasers and nanolasers remain largely unexplored, with few exceptions [13,18]. Here, we explore part of this new regime by showing that a simple microscopic laser geometry in which one mirror is realized by a Fano resonance, providing a so-called Fano laser (FL) [19,20], is intrinsically exceedingly stable toward external optical feedback, in some cases entirely suppressing coherence collapse. The origin of the strongly enhanced stability is identified as a unique reduction of the relaxation oscillation (RO) frequency, which suppresses a period-doubling route to chaos, and it is shown how the Fano laser outperforms lasers with conventional, nondispersive mirrors by orders of magnitude in terms of feedback stability. The Fano laser is analyzed using a generalization of the traditional Lang-Kobayashi model [5] for semiconductor lasers with external optical feedback.

Figure 1 shows schematic representations of the Fano laser and the conventional Fabry-Perot (FP) laser and their corresponding phase diagrams. The FL consists of a waveguide terminated at one end, which is side coupled to a nearby cavity, from whence the Fano interference between the continuum of waveguide modes and the discrete nanocavity mode leads to a narrow-band reflection peak [21,22] with the bandwidth inversely proportional to the quality factor of the nanocavity. This realizes a bound-mode-in-continuum [23], which functions as a cavity mode. This configuration was experimentally realized in a photonic crystal platform [20], showing remarkable properties including pinned single-mode lasing and the first case of self-pulsing in a microscopic laser [20,24], and theory suggests that its frequency modulation bandwidth is orders of magnitude larger than conventional lasers [25]. A comprehensive review of Fano lasers is given in [26]. The photonic crystal platform itself has provided numerous promising microscopic lasers for the photonic integrated circuits of the future [27–29].

Figures 1(b) and 1(d) show the calculated relative intensity noise (RIN) as a function of the external reflectivity $|r_3|^2$ and the distance to the external mirror L_D for a Fabry-Perot laser (top) and a Fano laser (bottom). The Fabry-Perot laser is described using the conventional Lang-Kobayashi model [5], while the Fano laser is modeled using a generalized version of the Lang-Kobayashi model, to be presented later. The RIN is defined as $\mathrm{RIN} = \delta P(t)^2/\langle P(t)\rangle^2$, where $\delta P(t)^2$ is the variance and $\langle P(t)\rangle$ is the mean of the time-domain output power. This provides a convenient quantitative measure of the stability, with low RIN (blue) indicating stable continuous-wave (cw) states and high RIN (yellow) corresponding to self-sustained oscillations, chaotic dynamics, and coherence collapse. Despite the intricacies of these phase diagrams, the main point is clear: The Fano laser provides an extraordinary improvement in feedback stability, as shown simply by comparing the sizes of the blue and yellow regions in Fig. 1. The critical feedback level, at which the laser is

 © 2019 American Physical Society

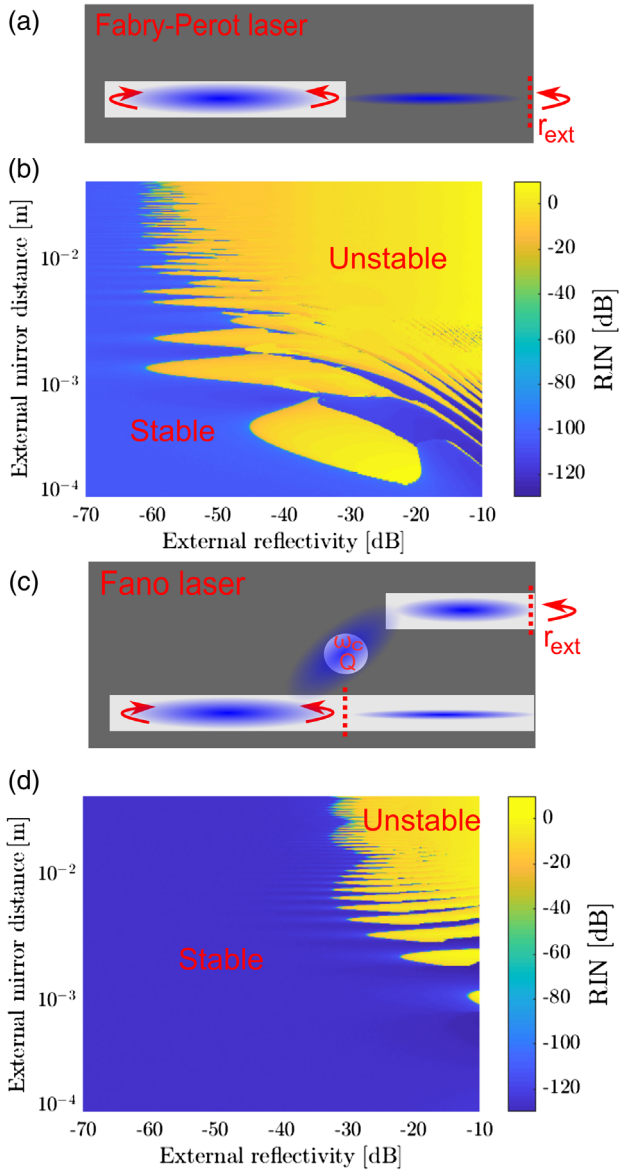

FIG. 1. (a) Schematic of Fabry-Perot laser. (b) RIN in decibels as function of external reflectivity and on-chip distance to the external mirror for the FP laser. (c) Schematic of Fano laser. (d) RIN as function of external reflectivity and on-chip distance to the external mirror for the Fano laser.

stable irrespective of the distance to the external reflector, is seen to be 3 orders of magnitude larger for the Fano laser compared to conventional lasers. Additionally, the Fano laser is essentially immune to feedback when the length scale reaches on-chip dimensions ($L_D \simeq 1$ mm), whereas this does not happen until $L_D \lesssim 100\ \mu$m for the Fabry-Perot laser. Furthermore, instabilities, chaos, and coherence collapse are completely suppressed for any feedback level for the Fano laser for certain ranges of delay lengths, a characteristic not observed for Fabry-Perot lasers. The Supplemental Material [30] presents a bifurcation analysis using Refs. [31–33], showing a period-doubling route to chaos for the Fano laser.

The phase diagram for the Fabry-Perot laser is generated using the conventional Lang-Kobayashi model for semiconductor lasers with external feedback [5]. This model has proven to work well for both Fabry-Perot and distributed feedback lasers, as well as vertical-cavity surface-emitting lasers [9], but in order to describe the Fano laser, a generalization is necessary. The generalization consists of coupling the Lang-Kobayashi model to a dynamical equation for the field stored in the nanocavity [19,24], in order to temporally resolve the Fano interference. This approach is also of interest for studying other coupled systems with complicated external feedback arrangements due to the generic nature of the formulation. As the output power is mainly coupled out through the cross port [19], the feedback is assumed to originate in this port, as illustrated in Fig. 1(c). This leads to the following model equations:

$$\frac{dA^+(t)}{dt} = \frac{1}{2}(1 - i\alpha)\left(\Gamma v_g g(N) - \frac{1}{\tau_p}\right)A^+(t) + \frac{1}{\tau_{\rm in}}A(t,\tau_D) + F_L(t), \tag{1}$$

$$\frac{dN(t)}{dt} = R_p - \frac{N}{\tau_s} - v_g g(N) N_p. \tag{2}$$

Here $A^+(t)$ is the envelope of the complex electric field in the laser cavity, $N(t)$ is the carrier density in the active region, α is the linewidth enhancement factor, and Γ is the field confinement factor. v_g is the group velocity, $g(N) = g_N(N - N_0)$ is the gain, with g_N being the differential gain and N_0 as the transparency carrier density, and τ_p is the photon lifetime. $\tau_{\rm in} = v_g/(2L)$ is the laser cavity round-trip time, with v_g being the group velocity and L as the cavity length, $F_L(t)$ is a complex Langevin noise source, R_p is the pump rate, and τ_s is a characteristic carrier lifetime. $N_p = \sigma_s |A^+(t)|^2/V_p$ is the photon density, where V_p is the photon volume and σ_s is given in Ref. [34]. Finally, $A(t,\tau_D)$ is related to the reflected external field and differs for the FP laser and the FL.

Lang-Kobayashi:

$$A(t,\tau_D) = \kappa A^+(t - \tau_D) e^{i\omega\tau_D}. \tag{3}$$

Fano Lang-Kobayashi:

$$A(t,\tau_D) = \frac{\sqrt{\gamma_c}}{r_2} A_c(t,\tau_D) - A^+(t) \tag{4}$$

$$\frac{dA_c(t,\tau_D)}{dt} = (-i\delta_c - \gamma_T)A_c(t) + i\sqrt{\gamma_c}A^+(t) - \gamma_{\rm cp} r_3 A_c(t - \tau_D) e^{i\omega\tau_D}. \tag{5}$$

Here $\kappa = (1 - |r_2|^2) r_3/|r_2|$ is the conventional definition of the external feedback coefficient [8], with r_2 and r_3

being the laser cavity and external mirror amplitude reflectivities, respectively. τ_D is the delay time of the external feedback and ω is the laser oscillation frequency. $A_c(t,\tau_D)$ is the field stored in the nanocavity, γ_c is the field coupling rate from the waveguide to the nanocavity, $\delta_c = \omega_c - \omega$ is the detuning of the resonance frequency of the nanocavity (ω_c) from the laser frequency, γ_T is the total decay rate of the nanocavity field, and $\gamma_{\rm cp}$ is the field coupling rate from the nanocavity into the cross port. For the FP laser, the external feedback enters directly into Eq. (1) [34], while for the FL it couples to Eq. (1) through the nanocavity field $A_c(t,\tau_D)$. This field is the solution to the conventional coupled-mode theory equation [21], but extended to self-consistently include the external feedback in Eq. (5). In the calculations, parameters appropriate for microscopic lasers are used, which by itself leads to a notably lower critical feedback level than is usually observed for macroscopic Fabry-Perot lasers. As the cavity length is in the few-micrometer range, the critical feedback level is ≈ -60 dB, which is orders of magnitude lower than the ≈ -40 dB observed for macroscopic lasers [8,9]. The parameters are given in the Supplemental Material [30], together with an efficient iterative formulation of the model equations.

We next turn to the physics responsible for the improved feedback stability of the Fano laser. The effect of the Fano mirror bandwidth is investigated in Fig. 2(a), showing the variation of the RIN with external reflectivity $|r_3|^2$ for a Fabry-Perot laser (circles) and Fano lasers with increasing values of the nanocavity Q factor for $\tau_D = 1$ ns. The four curves show the same qualitative shape, reflecting the phase diagrams of Fig. 1. The crucial difference between the curves, however, is the critical external reflectivity at which the onset of instability occurs, which varies by orders of magnitude. For low Q, the Fano laser RIN curve is close to the Fabry-Perot laser curve, and the critical feedback level then increases dramatically with the increase in quality factor, as shown in Fig. 2(b). From a stability analysis, one finds that in the short-cavity limit ($2Q_T/\omega \gg \tau_{\rm in}$) the Fano laser critical external reflectivity is given by

$$|r_{3C,\rm FL}|^2 = \left(\frac{2Q_T\gamma_{\rm FL}|r_2|}{\omega\sqrt{1+\alpha^2}(1-|r_2|^2)}\right)^2, \qquad (6)$$

where $\gamma_{\rm FL}$ is the Fano laser RO damping rate. This expression is plotted as the black line in Fig. 2(b), showing excellent agreement with the numerical results (red circles). Equation (6) is identical to that of Fabry-Perot lasers [35], except that half the laser round-trip time ($\tau_{\rm in}/2$) is replaced by $2Q_T/\omega$, i.e., the storage time of the energy in the nanocavity ($\tau_{p,\rm nc}$). Thus, the improvement in feedback stability is simply

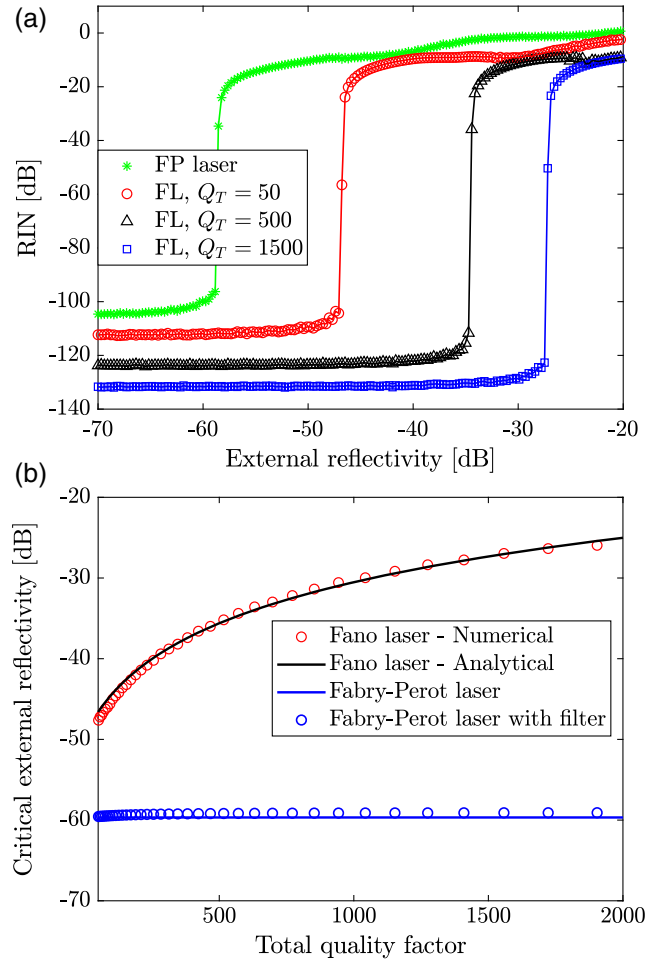

FIG. 2. (a) RIN as function of the external power reflectivity in decibels with $L_D = 3$ cm for a Fabry-Perot laser (stars) and Fano lasers with increasing nanocavity Q factors (circles, triangles, squares). Solid lines are guides to the eye. (b) Numerical (red circles) and analytical (black line) critical feedback level as function of the total quality factor of the nanocavity.

$$\Delta r_{3,C}[\rm dB] = 20\log_{10}\left(\frac{2\tau_{p,\rm nc}}{\tau_{\rm in}}\right), \qquad (7)$$

where $\Delta r_{3,C}$ is the difference in decibels between the critical external power reflectivity of a Fano laser and a Fabry-Perot laser with the same parameters. This shows how the improvement in stability is an intrinsic property of the Fano mirror, independent of all parameters other than the Q factor and the round-trip time.

The appearance of the Q factor as the governing parameter for the stability means the improvement is inversely proportional to the mirror linewidth, and as such, one might intuitively think that the Fano laser simply acts as a filter for the external feedback. Such filtered feedback systems are well studied, showing altered mode selection properties [36], changes to the laser dynamics [37], a sensitive dependence on the filter width [38], and phase-dependent stability improvements [39]. The blue circles in

Fig. 2(b) are a numerical calculation of the critical feedback level for a Fabry-Perot laser with filtered feedback, as a function of the filter width, showing how, in the range of relevant Q factors, the filtering is essentially broadband and negligible, so that the stability improvement of the Fano laser cannot be explained simply as a filtering effect. This is the case for the entire range of delay lengths covered in Fig. 1.

The improved stability can instead be understood by considering the paths to instability for lasers with feedback: Competition between allowed external cavity modes and relaxation oscillations becoming undamped through a Hopf bifurcation. The external cavity mode selection properties of Fano lasers in the presence of feedback differ fundamentally from conventional semiconductor lasers and instead function as an amplified version of the improved mode selection of lasers with filtered feedback [36]. For Fano lasers, the number of external cavity modes is strongly reduced due to the narrow bandwidth of the Fano mirror, which significantly increases the threshold gain of modes that are separated in frequency by more than $1/\gamma_T$. In this case, an effective C parameter [9] for the Fano laser may be estimated as

$$C_{\mathrm{FL}} = \kappa_{\mathrm{FL}} \frac{\tau_D}{\frac{2Q_T}{\omega} + \tau_{\mathrm{in}}} \sqrt{1+\alpha^2}, \tag{8}$$

where $\kappa_{\mathrm{FL}} = r_3(1-|r_2|) = r_3\gamma_{\mathrm{cp}}/\gamma_T$ acts as an effective feedback parameter for the Fano laser. In comparison to lasers with filtered feedback, the filtering of external cavity modes is much stronger, because a detuning in frequency changes the internal reflectivity of the laser, rather than simply the feedback strength, leading to a much larger threshold gain separation between neighboring external cavity modes. This extreme sensitivity to frequency changes ensures that a single, dominant external cavity mode is selected, so that the critical feedback level is uniquely determined by the location of the first Hopf bifurcation, and the location of this Hopf bifurcation is what is determined by Eq. (6).

The origin of the scaling with the Q factor in the expression for the critical feedback level is a unique reduction in the relaxation oscillation frequency for the Fano laser compared to Fabry-Perot lasers without notable change of the RO damping rate. The benefit of this reduction in terms of feedback stability is that the instability is born from ROs becoming undamped. Thus, if the frequency to damping rate ratio is reduced, fewer oscillations take place before a perturbation decays back to the steady state. Because of this, a larger level of feedback is necessary to drive the instability, leading to the feedback stability scaling with the Q factor. This type of reduction of the RO frequency is particularly efficient for suppressing coherence collapse, because the route to chaos is of the period-doubling form. As the temporal period is controlled by the RO frequency, a lower frequency means a longer period, requiring stronger feedback to sustain the oscillations through the longer and longer periods in order to drive the laser toward chaos. We believe that due to the generic nature of the FL equations and the stability mechanism, this type of behavior could also be exploited to suppress chaotic dynamics in other delay systems if the natural frequency of the system can be engineered, in particular for systems governed by period-doubling routes to chaos, as is the case here.

The reduction of the RO frequency with Q factor arises because of a longer effective photon lifetime of the system, as the high-Q nanocavity stores a significant amount of the intensity during lasing (see inset in Fig. 3). As the Q factor increases, this amount increases, as shown in Fig. 3 (right axis, blue curve), which in turn means that the interaction between photons and free carriers in the laser cavity is weaker, leading to a smaller relaxation oscillation frequency (full black, left axis), similar to reducing the photon number or increasing the photon lifetime of a conventional laser [40].

A small-signal analysis of the feedback-free FL equations yields the FL RO frequency as

$$\omega_{R,\mathrm{FL}}^2 = \omega_R^2 \left(1 - \frac{1}{1+\frac{\omega\tau_{\mathrm{in}}}{2Q_T}}\right). \tag{9}$$

Here ω_R is the corresponding RO frequency for a Fabry-Perot laser with the same parameters [40]. The connection to Eqs. (6) and (7) is clear, since in the short-cavity limit we have

$$\frac{\tau_{p,\mathrm{nc}}}{\tau_{\mathrm{in}}} = \frac{\omega_R^2}{\omega_{R,\mathrm{FL}}^2}, \tag{10}$$

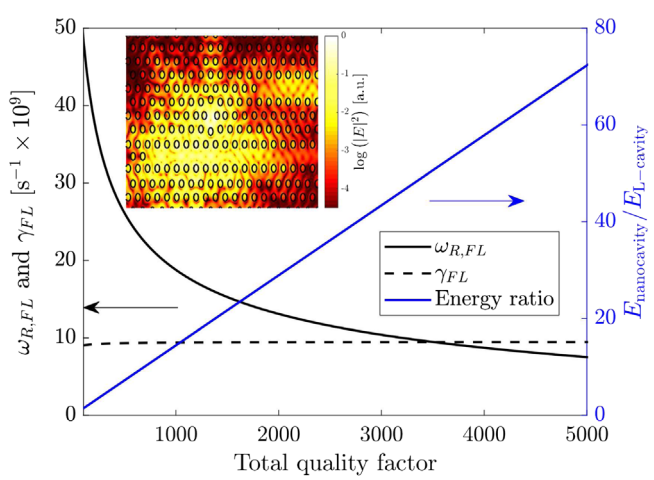

FIG. 3. Fano laser relaxation oscillation angular frequency (full black, left axis) and damping rate (dashed black, left axis), and ratio of energy stored in the nanocavity relative to the laser cavity (blue, right axis), all as a function of the total quality factor. (Inset) Simulated field distribution during lasing (logarithmic scale). Note the bright spots in the nanocavity.

showing how the reduction of the RO frequency explains the improved feedback stability.

Here, one should appreciate the fundamental difference between Fano and FP lasers. As additional energy is stored in the nanocavity due to the increasing Q factor, the RO frequency decreases until eventually the FL approaches an overdamped regime ($Q_T \gtrapprox 3500$). The absence of relaxation oscillations can be interpreted as a transition of the FL from a class B laser toward a class A laser [41], i.e., a system of lower dimensionality, which leads to an intrinsic suppression of chaos as the quality factor increases. For FP lasers, in contrast, the critical feedback level is determined exclusively by the damping rate [9], as exemplified by stability improvements due to a short carrier lifetime due to growth defects in Ref. [12]. Figure 3 shows that, despite the strong variation of the RO frequency, the Fano laser damping rate only changes marginally with Q. In contrast, the damping rate in conventional lasers increases approximately with the square of the RO frequency, showing how the mechanism of improved feedback stability in Fano lasers is fundamentally different.

In conclusion, it has been shown how semiconductor Fano lasers intrinsically suppress dynamic instabilities induced by exposure to external optical feedback. A generalization of the Lang-Kobayashi model was employed to study the laser dynamics. Using this, the feedback stability was analytically and numerically shown to scale with the quality factor of the nanocavity, due to a unique reduction of the relaxation oscillation frequency, as well as large gain separation of external cavity modes due to the highly dispersive Fano mirror. For realistic designs, the Fano laser outperforms conventional Fabry-Perot lasers by orders of magnitude in terms of the critical external feedback level. In many cases, coherence collapse is even entirely suppressed, in contrast to the conventional classification of semiconductor lasers with feedback, demonstrating fundamentally new and different underlying dynamics arising from the Fano mirror. Because of the general nature of the problem, this stability mechanism may be exploitable for chaos suppression in similar delay systems.

Authors gratefully acknowledge funding by Villum Fonden via the NATEC Center of Excellence (Grant No. 8692). This project has received funding from the European Research Council (ERC) under the European Union's Horizon 2020 Research and Innovation Programme (Grant No. 834410 FANO).

*thsv@fotonik.dtu.dk
†yiyu@fotonik.dtu.dk
‡jesm@fotonik.dtu.dk

[1] J. D. Farmer, Chaotic attractors of an infinite-dimensional dynamical system, Physica (Amsterdam) **4D**, 366 (1982).
[2] H. Y. Hu and Z. H. Wang, *Dynamics of Controlled Mechanical Systems with Delayed Feedback* (Springer Science +Business Media, Berlin, 2013).
[3] M. C. Mackey and L. Glass, Oscillation and chaos in physiological control systems, Science **197**, 287 (1977).
[4] T.-L. Liao and F.-C. Wang, Global stability for cellular neural networks with time delay, IEEE Trans. Neural Networks **11**, 1481 (2000).
[5] R. Lang and K. Kobayashi, External optical feedback effects on semiconductor injection laser properties, IEEE J. Quantum Electron. **16**, 347 (1980).
[6] D. Lenstra, B. Verbeek, and A. Den Boef, Coherence collapse in single-mode semiconductor lasers due to optical feedback, IEEE J. Quantum Electron. **21**, 674 (1985).
[7] J. Mørk, J. Mark, and B. Tromborg, Route to Chaos and Competition between Relaxation Oscillations for a Semiconductor Laser with Optical Feedback, Phys. Rev. Lett. **65**, 1999 (1990).
[8] J. Mork, B. Tromborg, and J. Mark, Chaos in semiconductor lasers with optical feedback: Theory and experiment, IEEE J. Quantum Electron. **28**, 93 (1992).
[9] K. Petermann, External optical feedback phenomena in semiconductor lasers, IEEE J. Sel. Top. Quantum Electron. **1**, 480 (1995).
[10] M. Sciamanna and K. A. Shore, Physics and applications of laser diode chaos, Nat. Photonics **9**, 151 (2015).
[11] M. J. Wishon, A. Locquet, C. Y. Chang, D. Choi, and D. S. Citrin, Crisis route to chaos in semiconductor lasers subjected to external optical feedback, Phys. Rev. A **97**, 033849 (2018).
[12] H. Huang, J. Duan, D. Jung, A. Y. Liu, Z. Zhang, J. Norman, J. E. Bowers, and F. Grillot, Analysis of the optical feedback dynamics in InAs/GaAs quantum dot lasers directly grown on silicon, J. Opt. Soc. Am. B **35**, 2780 (2018).
[13] P. Munnelly, B. Lingnau, M. M. Karow, T. Heindel, M. Kamp, S. Höfling, K. Lüdge, C. Schneider, and S. Reitzenstein, On-chip optoelectronic feedback in a micropillar laser-detector assembly, Optica **4**, 303 (2017).
[14] T. T. M. van Schaijk, D. Lenstra, E. A. J. M. Bente, and K. A. Williams, Rate-equation theory of a feedback insensitive unidirectional semiconductor ring laser, Opt. Express **26**, 13361 (2018).
[15] K. Takata and M. Notomi, Photonic Topological Insulating Phase Induced Solely by Gain and Loss, Phys. Rev. Lett. **121**, 213902 (2018).
[16] L. Lu, J. D. Joannopoulos, and M. Soljacic, Topological photonics, Nat. Photonics **8**, 821 (2014).
[17] J. Duan, H. Huang, Z. G. Lu, P. J. Poole, C. Wang, and F. Grillot, Narrow spectral linewidth in InAs/InP quantum dot distributed feedback lasers, Appl. Phys. Lett. **112**, 121102 (2018).
[18] T. Wang, X. Wang, Z. Deng, J. Sun, G. P. Puccioni, G. Wang, and G. L. Lippi, Dynamics of a micro-VCSEL operated in the threshold region under low-level optical feedback, IEEE J. Sel. Top. Quantum Electron. **25**, 1 (2019).
[19] J. Mork, Y. Chen, and M. Heuck, Photonic Crystal Fano Laser: Terahertz Modulation and Ultrashort Pulse Generation, Phys. Rev. Lett. **113**, 163901 (2014).

[20] Y. Yu, W. Xue, E. Semenova, K. Yvind, and J. Mork, Demonstration of a self-pulsing photonic crystal Fano laser, Nat. Photonics **11**, 81 (2017).

[21] S. Fan, W. Suh, and J. D. Joannopoulos, Temporal coupled-mode theory for the Fano resonance in optical resonators, J. Opt. Soc. Am. A **20**, 569 (2003).

[22] A. E. Miroshnichenko, S. Flach, and Y. S. Kivshar, Fano resonances in nanoscale structures, Rev. Mod. Phys. **82**, 2257 (2010).

[23] C. W. Hsu, B. Zhen, A. D. Stone, J. D. Joannopoulos, and M. Soljacic, Bound states in the continuum, Nat. Rev. Mater. **1**, 16048 (2016).

[24] T. S. Rasmussen, Y. Yu, and J. Mork, Theory of self-pulsing in photonic crystal Fano lasers, Laser Photonics Rev. **11**, 1700089 (2017).

[25] T. S. Rasmussen, Y. Yu, and J. Mork, Modes, stability, and small-signal response of photonic crystal Fano lasers, Opt. Express **26**, 16365 (2018).

[26] J. Mork, Y. Yu, T. S. Rasmussen, E. Semenova, and K. Yvind, Semiconductor Fano lasers, IEEE J. Sel. Top. Quantum Electron. **25**, 1 (2019).

[27] S. Matsuo, T. Sato, K. Takeda, A. Shinya, K. Nozaki, H. Taniyama, M. Notomi, K. Hasebe, and T. Kakitsuka, Ultralow operating energy electrically driven photonic crystal lasers, IEEE J. Sel. Top. Quantum Electron. **19**, 4900311 (2013).

[28] G. Crosnier, D. Sanchez, S. Bouchoule, P. Monnier, G. Beaudoin, I. Sagnes, R. Raj, and F. Raineri, Hybrid indium phosphide-on-silicon nanolaser diode, Nat. Photonics **11**, 297 (2017).

[29] Y. Ota, M. Kakuda, K. Watanabe, S. Iwamoto, and Y. Arakawa, Thresholdless quantum dot nanolaser, Opt. Express **25**, 19981 (2017).

[30] See Supplemental Material at http://link.aps.org/supplemental/10.1103/PhysRevLett.123.233904 for an outline of the computational model and parameters, and a bifurcation analysis of the route to chaos.

[31] R. Tkach and A. Chraplyvy, Regimes of feedback effects in 1.5-um distributed feedback lasers, J. Lightwave Technol. **4**, 1655 (1986).

[32] T. Heil, I. Fischer, W. Elsäßer, and A. Gavrielides, Dynamics of Semiconductor Lasers Subject to Delayed Optical Feedback: The Short Cavity Regime, Phys. Rev. Lett. **87**, 243901 (2001).

[33] J. Mork, B. Tromborg, and P. L. Christiansen, Bistability and low-frequency fluctuations in semiconductor lasers with optical feedback: A theoretical analysis, IEEE J. Quantum Electron. **24**, 123 (1988).

[34] B. Tromborg, H. Olesen, X. Pan, and S. Saito, Transmission line description of optical feedback and injection locking for Fabry-Perot and dfb lasers, IEEE J. Quantum Electron. **23**, 1875 (1987).

[35] B. Tromborg and J. Mork, Nonlinear injection locking dynamics and the onset of coherence collapse in external cavity lasers, IEEE J. Quantum Electron. **26**, 642 (1990).

[36] M. Yousefi and D. Lenstra, Dynamical behavior of a semiconductor laser with filtered external optical feedback, IEEE J. Quantum Electron. **35**, 970 (1999).

[37] A. Fischer, M. Yousefi, D. Lenstra, M. W. Carter, and G. Vemuri, Experimental and theoretical study of semiconductor laser dynamics due to filtered optical feedback, IEEE J. Sel. Top. Quantum Electron. **10**, 944 (2004).

[38] H. Erzgräber and B. Krauskopf, Dynamics of a filtered-feedback laser: Influence of the filter width, Opt. Lett. **32**, 2441 (2007).

[39] V. Z. Tronciu, H.-J. Wünsche, M. Wolfrum, and M. Radziunas, Semiconductor laser under resonant feedback from a Fabry-Perot resonator: Stability of continuous-wave operation, Phys. Rev. E **73**, 046205 (2006).

[40] L. Coldren and S. Corzine, *Diode Lasers and Photonic Integrated Circuits*, 1st ed. (Wiley, New York, 1995).

[41] J. R. Tredicce, F. T. Arecchi, G. L. Lippi, and G. P. Puccioni, Instabilities in lasers with an injected signal, J. Opt. Soc. Am. B **2**, 173 (1985).